Pergamon

Ultrasound in Med. & Biol., Vol. 21, No. 7, pp. 937–944, 1995

0301-5629/95 $9.50 + .00

0301-5629(95)00039-9

●*Original Contribution*

VELOCITY MATCHED SPECTRUM ANALYSIS: A NEW METHOD FOR SUPPRESSING VELOCITY AMBIGUITY IN PULSED-WAVE DOPPLER

HANS TORP[†] and KJELL KRISTOFFERSEN[‡]

[†]Department of Biomedical Engineering, University of Trondheim, Trondheim, Norway; and [‡]Vingmed Sound A/S, Oslo, Norway

(*Received* 5 *December* 1995; *in final form* 6 *March* 1995)

Abstract—A new approach to spectrum analysis, which is capable of suppressing velocity ambiguity in pulsed-wave ultrasonic Doppler, is presented. By simultaneous processing of several data samples from a range in depth, the movement of the scatterers along the ultrasonic beam can be tracked from pulse to pulse for each velocity component in the spectrum. In this way the correlation length of the signal component arising from a specific velocity increases when that velocity matches the expected velocity. The resulting velocity/time spectral display shows a more clearly defined spectral envelope of the maximum velocity than with conventional methods based on the discrete Fourier transform of the Doppler signal. This makes it possible to delineate velocity waveforms with peak velocity up to several times the Nyquist limit. Experimental data from human subclavian and aortic arteries are presented, where the new method is compared to conventional spectrum analysis.

Key Words: **Pulsed Doppler ultrasound, Doppler signal processing, Spectrum analysis, Blood flow.**

INTRODUCTION

Spectrum analysis based on the modified periodogram method (Oppenheim and Schafer 1975), as well as parametric spectrum estimation algorithms, have been the commonly used methods for generating velocity/time waveforms in ultrasound Doppler blood flow measurements. With this technique, moderate frequency aliasing can be compensated for by baseline shift, as long as the maximum frequency shift is lower than two times the Nyquist limit. In principle, a smoothly varying velocity curve can be followed through several "wraparounds" by stacking several equal sonograms at the top of each other (Iinuma 1984; Kristoffersen 1984). Two factors limit the use of this technique:

1. The transit-time effect due to limited pulse length increases the spectral bandwidth which destroys the spectral envelope for high velocities.
2. The high-pass filter used for wall motion rejection blanks out the spectrum in an area close to each multiple of the sampling frequency.

Address correspondence to: Hans Torp, Department of Biomedical Engineering, Medical Technical Research Center, University of Trondheim, N-7005 Trondheim, Norway. E-mail: hans.torp@ibt.unit.no

Several different methods have been proposed for resolving velocity ambiguity arising in pulsed-wave Doppler measurements. Bonnefous and Pesque (1986) estimated pulse-to-pulse time shift by searching for the shift which gave maximum correlation between two consecutive radiofrequency (RF) echo signals. This method gives a good estimate of blood flow velocity when the velocity distribution is narrow, and velocity ambiguity can be resolved when the pulse bandwidth is sufficiently high.

Another approach was used by Ferrara and Algazi (1991, 1992). From a stochastic model of the signal from a point scatterer, a maximum likelihood estimator for the velocity was derived. The velocity likelihood function used in their "point target ML estimator" is based on the same principles as the method presented in this work. A similar approach has been taken by Wilson (1991), in which a matched filter for each velocity is found by integrating the received RF data along straight lines in the depth/time plane. He shows that this is equivalent to an integration along a straight line in the two-dimensional (2D) Fourier plane.

The methods listed above give only the mean velocity and the velocity spread, which is what is needed for color flow imaging display. However, quantitative

velocity information, like the spatial maximum velocity, cannot be obtained in this way, unless the velocity field is constant through the entire sample volume. Doppler spectrum analysis with a velocity–time display has proven to be the most robust and accurate way of presenting quantitative blood velocity information.

In this article, a method which suppresses frequency aliasing in the Doppler spectrum velocity–time display is presented. First, a review of a signal model is given, which characterizes the signal by a 2D power spectrum. Then the new spectrum algorithm is described, including its interpretation in the 2D Fourier plane. The method is denoted "velocity matched spectrum" (VM spectrum), since the spectral window matches the 2D spectrum for each blood velocity component. The performance of the VM-spectrum estimator is analyzed theoretically, showing suppression of side lobes and grating lobes compared to the conventional spectral estimator. Experimental results are shown, in which the algorithm is applied to recorded ultrasonic RF data from human arteries.

SIGNAL MODEL

The presented method for spectrum analysis utilizes the correlation in the signal between samples in depth over time caused by the movement of the blood scatterers. Therefore, a signal model which includes correlation both in range and time (between consecutive pulses) is useful in describing its properties. Similar models have been presented by a number of authors (Angelsen 1980; Mo and Cobbold 1992; Wilson 1991). Here, the model description is taken from a previous work (Torp et al. 1994), in which the received signal after complex demodulation and low-pass filtering is described as a 2D complex Gaussian process $x(t, k)$. In this notation, t is the elapsed time from pulse transmission, k, corresponding to a depth range, $r = \frac{c}{2}t$. In a practical implementation, the signal in digital form is only available for discrete samples in range. Conventional pulsed Doppler algorithms require only one range sample for each transmitted pulse, whereas the velocity matched algorithm uses a number of samples over a certain depth range. The receiver bandwidth is in most cases matched to the bandwidth of the transmitted pulse to limit thermal noise without increasing the sample volume in the radial direction. If the signal is sampled with a frequency higher than twice the bandwidth, any value in between can be found by interpolation. In the following analysis, the signal is assumed to be a continuous function of t, the elapsed time after pulse transmission. As a complex Gaussian process, the signal is completely characterized by its autocorrelation function, or the power spectrum, defined as

$$R_x(\tau, m) \equiv \langle x(t, k) * x(t + \tau, k + m) \rangle \quad (1)$$

The autocorrelation function in eqn (1) is defined by the statistical ensemble average of the signal product. In a practical estimator, ensemble averaging must be replaced by radial and/or temporal (pulse-to-pulse) averaging, to reduce variance.

In some of the expressions below, it is more convenient to use the complex pre-envelope of the received signal $x_p(t, k) = x(t, k)e^{i\omega_0 t}$, where ω_0 is the angular demodulation frequency. The autocorrelation function, and the corresponding power spectrum for the complex pre-envelope signal, is given by

$$R_{x_p}(\tau, m) \equiv \langle x_p(t, k) * x_p(t + \tau, k + m) \rangle = R_x(\tau, m)e^{i\omega_0 \tau}$$

$$G(\omega_1, \omega_2) \equiv \sum_m \int d\tau R_{x_p}(\tau, m)e^{i\omega_1 \tau}e^{i\omega_2 mT} \quad (2)$$

Note that the power spectrum is defined in the usual way as the 2D Fourier transform of the autocorrelation function. Due to the sampled nature of the Doppler signal, the power spectrum $G(\omega_1, \omega_2)$ is periodic in the ω_2 variable, and may therefore be written as a sum of copies of the nonaliased part $G_0(\omega_1, \omega_2)$, with distances equal to the angular pulse repetition frequency $2\pi/T$. The pulse repetition period is T.

$$G(\omega_1, \omega_2) = \sum_n G_0\left(\omega_1, \omega_2 + n\frac{2\pi}{T}\right)$$

$$G_0(\omega_1, \omega_2) \equiv \int dm \int d\tau R_{x_p}(\tau, m)e^{i\omega_1 \tau}e^{i\omega_2 mT} \quad (3)$$

The autocorrelation function is determined by the point echo response from blood, $s(t)$ (including frequency-dependent attenuation and scattering), and the transversal two-way beam sensitivity function, $b(d)$, where d is the distance from the ultrasonic beam center axis. If the blood velocity field is stationary and uniform, the autocorrelation function takes on the form

$$R_{x_p}(\tau, m; v_r, v_t) = s_2(\tau - m\delta_{v_r}) \cdot b_2(v_t Tm)$$

$$\delta_{v_r} = -\frac{2v_r T}{c} \quad (4)$$

where v_r and v_t are the velocity components in the radial

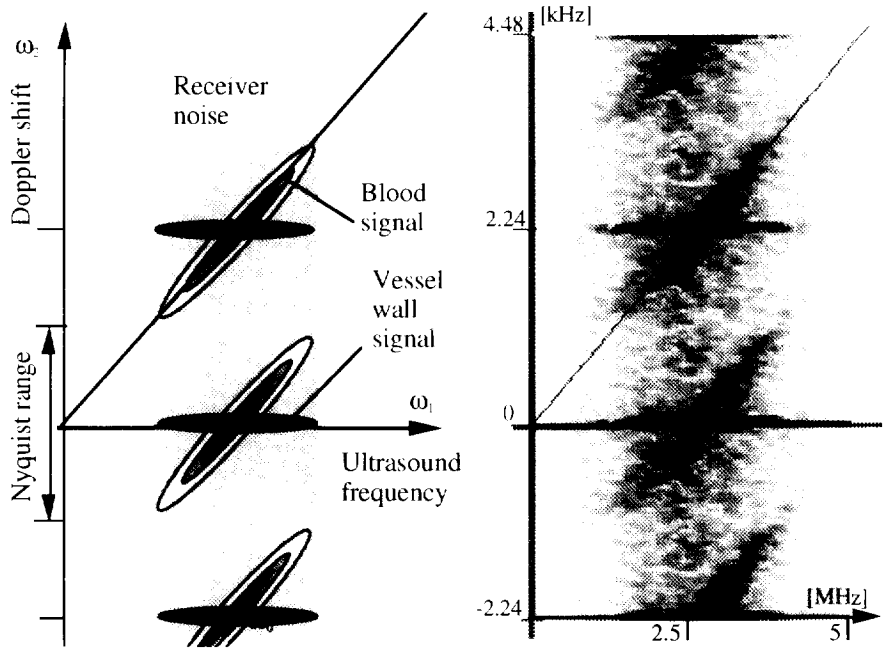

Fig. 1. The 2D spectrum of a blood flow signal including low frequency components from vessel walls, and thermal receiver noise. To the right the measured 2D spectrum of a signal from a normal human artery is shown.

(along the ultrasonic beam) and lateral (transversal to the ultrasonic beam) direction. Subscripts s_2 and b_2 indicate short notation for the autocorrelation operator applied to s and b, respectively; T is the pulse repetition period, and c is the speed of sound. The radial velocity component causes a change in arrival time from pulse to pulse, denoted δ_v. The minus sign in eqn (2) is due to the convention that positive velocity suggests "in the direction of" the transducer.

The nonaliased part of the spectrum $G_0(\omega_1, \omega_2)$ is obtained by combining eqns (3) and (4)

$$G_0(\omega_1, \omega_2) = |S(\omega_1)|^2 \cdot \left| B\left(\frac{1}{v_t}\left(\omega_2 - \frac{2v_t}{c}\omega_1\right)\right)\right|^2 \quad (5)$$

where $S(\omega_1)$ and $B(\omega_2)$ are the Fourier transforms of s and b, respectively. The frequency response $S(\omega_1)$ limits the spectral bandwidth in the ω_1 direction. The argument of B is zero along a straight line through the origin in the (ω_1, ω_2) plane, which represents the Doppler shift equation. Since B is a low-pass function, the spectral energy is concentrated along this line, and the bandwidth in the ω_2-direction is proportional to the lateral velocity component. In a general nonuniform velocity field, the signal power spectrum can be obtained by integrating the spectrum in eqn (5) over the velocity distribution inside the ultrasonic beam.

In Fig. 1, the 2D power spectrum is shown for ultrasound RF signals from a human artery, comprising the vessel wall signal with low Doppler shift, blood signal with Doppler shift equal to the pulse repetition frequency and thermal noise from the receiver front-end. Note that the spectral components for blood can be clearly distinguished from the vessel wall signal, although the mean Doppler frequency shift is close to zero for both signal components.

ESTIMATE OF THE VELOCITY SPECTRUM

The 2D power spectrum display in Fig. 1 can be used for quantitative velocity measurements by measuring the slope of a straight line through the origin, manually drawn to fit the spectrum. This will give the velocity at one time instant, but it is not a practical method to construct velocity–time graphs. By integrating the 2D power spectrum along lines through the origin for a number of predefined velocity values, a velocity spectrum with suppressed aliasing can be constructed. An algorithm based on this principle has been proposed by Wilson (1991). It turns out that this is equivalent to summation of the signal along skewed lines in the range/time plane, where the slope is chosen to follow the movement of the scatterers along the ultrasonic beam for each velocity in the spectrum. When the slope matches the actual velocity, the received echoes will match both in phase and amplitude, giving a peak in the spectrum at the actual velocity value. This principle is illustrated in Fig. 2. The velocity spectrum $p(v)$ can be calculated from the pre-

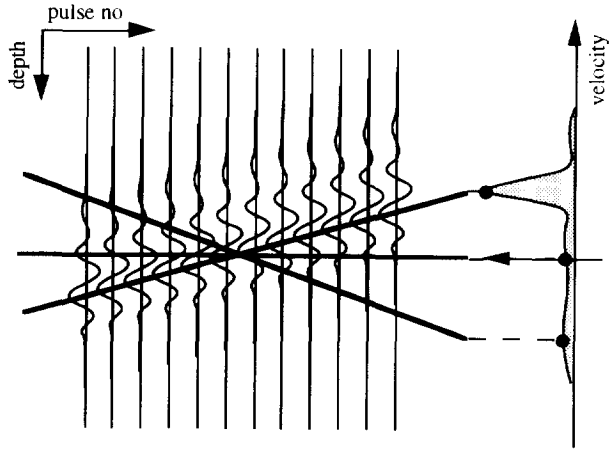

Fig. 2. The VM spectrum is obtained by a summation of the RF pre-envelope signal along skewed lines in time (or pulse no.) and depth range. The resulting spectrum is shown to the right.

envelope, $x_p(t, k)$, or from the complex (base-band) envelope, $x(t, k)$. The corresponding expression for a conventional spectrum, based on the modified periodogram method, is denoted $p_{\text{conv.}}(v)$

$$\hat{p}(v) = \left| \sum_k w(k) x_p(t_0 + k\delta, k_0 + k) \right|^2$$

$$= \left| \sum_k w(k) x(t_0 + k\delta, k_0 + k) e^{i\omega_0 k\delta} \right|^2$$

$$\hat{p}_{\text{conv.}}(v) = \left| \sum_k w(k) x_p(t_0, k_0 + k) e^{i\omega_0 k\delta} \right|^2$$

$$= \left| \sum_k w(k) x(t_0, k_0 + k) e^{i\omega_0 k\delta} \right|^2$$

$$\delta = 2T \frac{v}{c} \tag{6}$$

Here, $w(k)$ denotes the window function, which may be a rectangular or a smooth window (Hanning, Hamming, *etc.*). Note that the conventional spectrum estimator uses only one sample in the range direction, whereas the velocity matched (VM) spectrum uses several samples over a depth range which increases proportional to the velocity, v. The expected value of the two velocity spectrum estimators in eqn (6) can be expressed by the 2D autocorrelation function, defined in eqn (2).

$$\langle \hat{p}(v) \rangle = \sum_m w_2(m) R_{x_p}(m\delta, m)$$

$$\langle \hat{p}_{\text{conv.}}(v) \rangle = \sum_m w_2(m) R_{x_p}(0, m) e^{i\omega_0 m\delta}$$

$$w_2(m) = \sum_n w(n) w(n + m) \tag{7}$$

The expected value of the velocity spectrum estimators can also be expressed by the 2D power spectrum, and the Fourier transform $W(\cdot)$ of the window function, $w(k)$, by combining eqns (2) and (7).

$$\langle \hat{p}(v) \rangle = \iint d\omega_1 d\omega_2 G(\omega_1, \omega_2) \left| W\left(T\omega_2 - \frac{2vT}{c} \omega_1 \right) \right|^2$$

$$\langle \hat{p}_{\text{conv}}(v) \rangle = \iint d\omega_1 d\omega_2 G(\omega_1, \omega_2) \left| W\left(T\omega_2 - \frac{2vT}{c} \omega_0 \right) \right|^2 \tag{8}$$

Both spectrum estimators in eqn (8) have the form of an integral of the 2D power spectrum, weighted by a velocity-dependent spectral window function. An illustration of the spectral window function for the conventional spectrum compared to the VM spectrum is shown in Fig. 3. The spectral window for the VM spectrum is centered around the Doppler equation line, with a vertical width equal to the bandwidth of the window function, $w(k)$. The velocity spectrum is obtained by rotating the spectral window with a fixed point in the origin. For the conventional spectrum, the 2D spectral window has the same vertical width, but the slope is horizontal, and the velocity spectrum is obtained by translating the window in the vertical direction. The expected velocity spectrum for a uniform velocity field with direction θ and velocity components $v_r = v_0$, $v_t = v_0 \tan(\theta)$ is obtained by combining eqns (4) and (8)

$$\langle \hat{p}(v | v_0) \rangle = \sum_m w_2(m) s_2\left(\frac{2T}{c} m(v - v_0) \right) b_2(m v_0 \tan(\theta) T)$$

$$\langle \hat{p}_{\text{conv.}}(v | v_0) \rangle = \sum_m w_2(m) s_2\left(\frac{2T}{c} m v_0 \right) b_2(m v_0 \tan(\theta) T) e^{i\omega_0 m\delta} \tag{9}$$

If the flow direction is axial, *i.e.*, $\theta = 0$, the last term

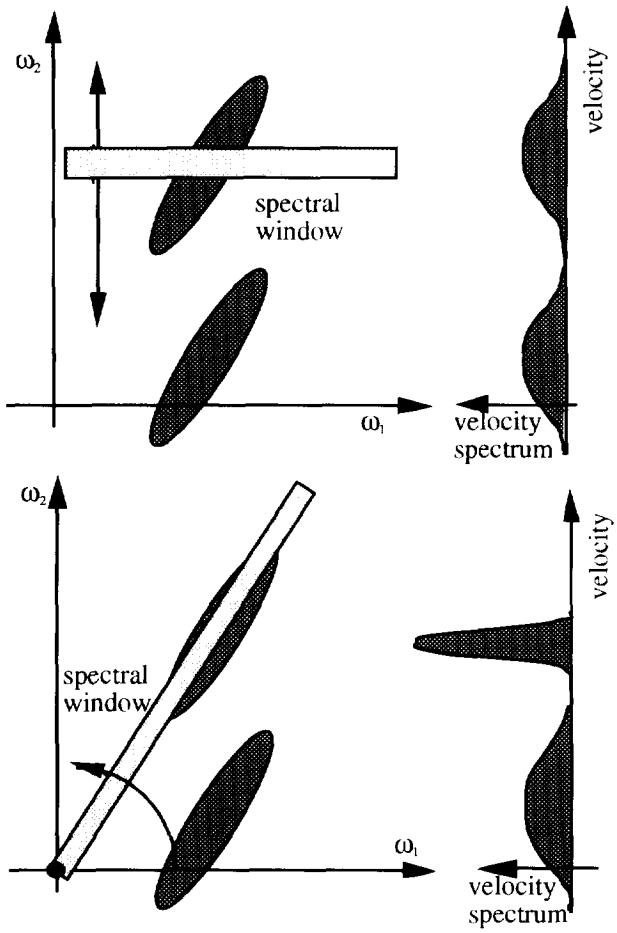

Fig. 3. Data window in the 2D Fourier domain for the conventional spectrum (upper diagram), and the velocity matched spectrum (lower diagram). The corresponding velocity spectra are shown to the right.

in eqn (9) equals the constant $b_2(0)$. In eqn (11), the expected value for the velocity matched spectrum and the conventional spectrum are expressed in the time and frequency domain.

$$\langle \hat{p}(v|v_0)\rangle = \sum_m w_2(m)s_2\left(\frac{2T}{c}m(v - v_0)\right)$$

$$= \int d\omega_1 |S(\omega_1)|^2 \left|W\left(\frac{2T}{c}(v - v_0)\omega_1\right)\right|^2$$

$$\langle \hat{p}_{\text{conv.}}(v|v_0)\rangle$$

$$= \int d\omega_1 |S(\omega_1)|^2 \left|W\left(\frac{2T}{c}(v_0\omega_1 - v\omega_0)\right)\right|^2 \quad (10)$$

In Fig. 4, the two spectral estimators are compared for $v = 0$ and $v = 2$ times the Nyquist limit, using eqn (10). Note that the VM spectrum estimator is translation invariant in the velocity v_0. This is not the case for the conventional spectrum, where the transit time broadening increases proportionally to the velocity. For the VM algorithm, the data window along the beam is matched to the velocity, and thus no additional transit-time broadening occurs for higher velocities. The main lobe and the near side lobes are determined by the window frequency response $W(\omega)$, whereas the grating lobe width is determined by the pulse bandwidth. For narrow-pulse bandwidth, the grating lobes are equal to the main lobe; increasing bandwidth gives lower peak values and larger width. For the numerical example shown in Fig. 4, the conventional spectrum analysis gives a much broader main lobe than the VM spectrum when the blood velocity equals the double Nyquist limit; see lower part of Fig. 4.

If the blood flow direction angle θ is different from zero, or the velocity field is nonuniform due to velocity gradients inside the ultrasonic beam, the main lobe in the spectrum will broaden. This effect is the same for both the conventional spectrum and the VM spectrum.

Frequency-dependent attenuation and scattering will change the center frequency of the received signal, and give a calibration error in the conventional Doppler spectrum. In the expressions above, the center frequency is assumed to be equal to the demodulation mixer frequency, ω_0, which may give a substantial bias in the conventional velocity spectrum if the transmitted pulse bandwidth is high. However, the expected value of the VM spectrum is independent of ω_0 [see eqns (9) and (11)], and frequency-dependent attenuation will therefore give no bias.

EXPERIMENTS AND DISCUSSION

In vivo experiments were performed using a commercial ultrasound scanner (Vingmed CFM 750) with spectral Doppler and color Doppler facilities. Some modifications were done to increase the bandwidth of the transmitted pulse and the receiver front-end amplifier. Unprocessed RF data were collected in real time with a custom 12-bit, 10-MHz digitizer and storage device, and transferred to a Mac II computer for disc storage, processing and display. We used a 3.25-MHz annular array transducer, with a transmitting frequency of 2.5 MHz. Data were collected from a normal human subclavian artery and aortic artery in a 10-mm depth range located 5 to 6 cm from the transducer, in approximately 1 s, to get one full heart cycle of data. The mean frequency and bandwidth of the received signal was measured by standard spectrum analysis methods,

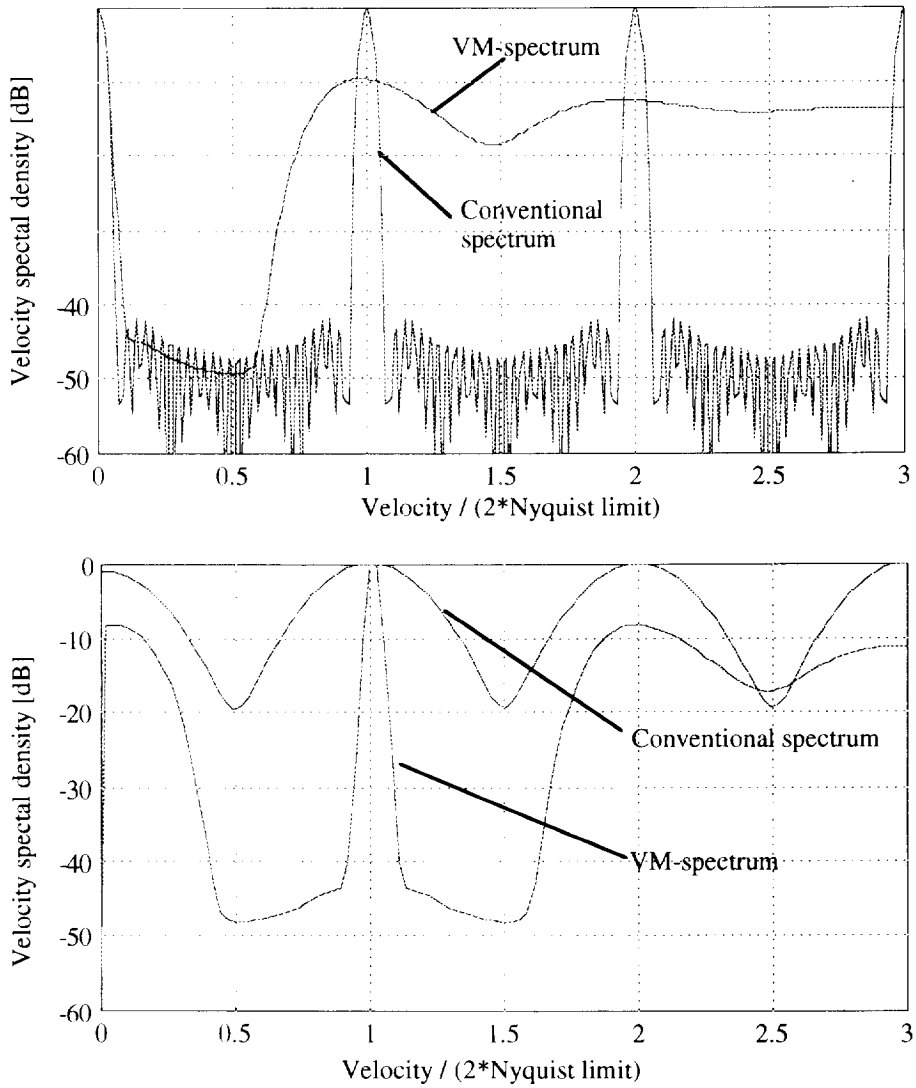

Fig. 4. Theoretical performance of the VM spectrum compared to conventional spectrum with laminar, axial flow with velocity $v = 0$ (upper plot), and $v = 2$ times the Nyquist limit (lower plot).

giving $f_0 = 2.55$ MHz, and -6-dB bandwidth equal to 1.34 MHz, *i.e.*, a fractional bandwidth of 53%. The data were processed off-line using standard methods for quadrature demodulation and wall motion rejection filtering. The radial sampling frequency was kept at 10 MHz after quadrature demodulation.

Doppler spectrum analysis was performed on the complex demodulated data, using both the conventional algorithm, and the VM algorithm, as described in eqn (6). The window function, $w(k)$, was a 32-point Hamming window. For the highest velocity values in the spectrum, the window length had to be reduced not to exceed the 10-mm-long depth range of available data. Since the complex demodulated data were highly oversampled (10-MHz sampling frequency, and 1.34-MHz bandwidth), no radial interpolation in the data was performed; the closest sample in range was selected according to eqn (6). In Figs. 5, 6 and 7, spectrum displays are shown for three different sets of RF data collected from normal human arteries. Conventional spectrum analysis is shown on the left, and VM spectrum analysis is shown on the right. Note that the same RF data and wall filter are used for both methods; however, as pointed out in the previous section, the VM spectrum algorithm utilizes data from several samples in the range direction, in contrast to the conventional spectrum algorithm. The pulse repetition frequency (PRF) was adjusted downward to obtain different degrees of spectral aliasing. In Figs. 5 and 6 PRF = 2.24 kHz, and in Fig. 7 PRF = 1.12 kHz, giving aliasing varying from 2 up to 4.5 times the Nyquist limit.

Thus, the following observations were drawn:

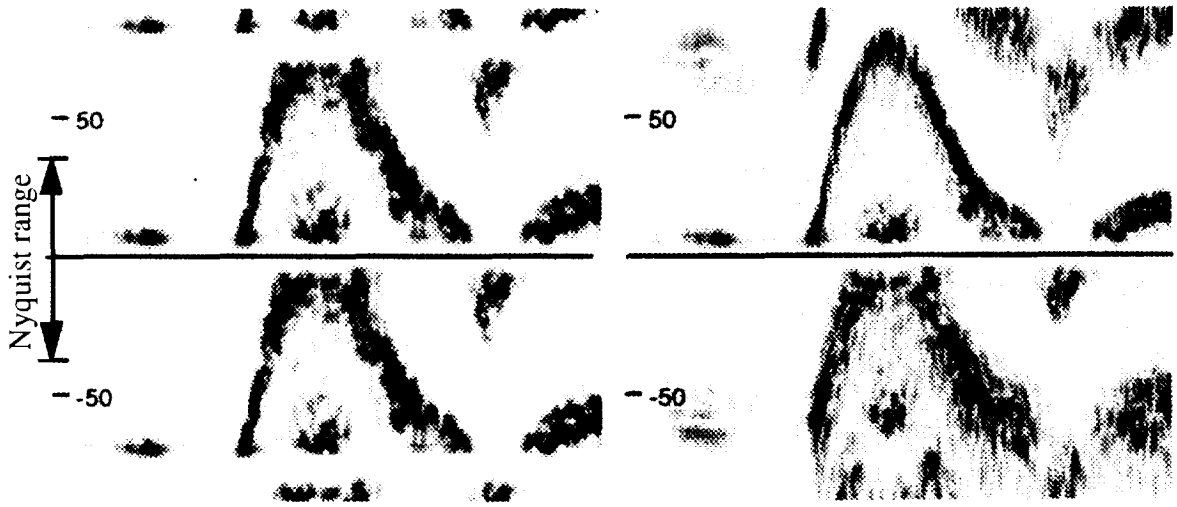

Fig. 5. VM spectrum analysis (right) compared to conventional spectrum analysis (left) applies to signals from a normal human subclavian artery with peak velocity at two times the Nyquist limit. Velocity labels are in centimeters per second.

1. In all three examples the "correct" velocity waveform stands out more clearly in the display for the VM-algorithm, than for the conventional algorithm. The spectral width is narrow close to the correct velocity, and is "smeared out" at the aliased parts; Fig. 7 shows this effect most clearly. This property was predicted from the theoretical calculations in the previous section (see Fig. 4).
2. The rejected bands in the spectrum around each multiple of the sampling frequency due to the wall motion rejection filter, which can be seen in the left-hand diagrams, are almost eliminated with the velocity matched algorithm shown in the right-hand diagrams. This is clearly demonstrated in Fig. 5, at the peak systole, where the spectrum envelope is destroyed by the wall motion filter for the conventional algorithm. The effect can be explained by the difference in the geometrical form of the 2D spectral window functions (see Fig. 3). The spectral window for the VM algorithm is tilted, and will therefore pick up some

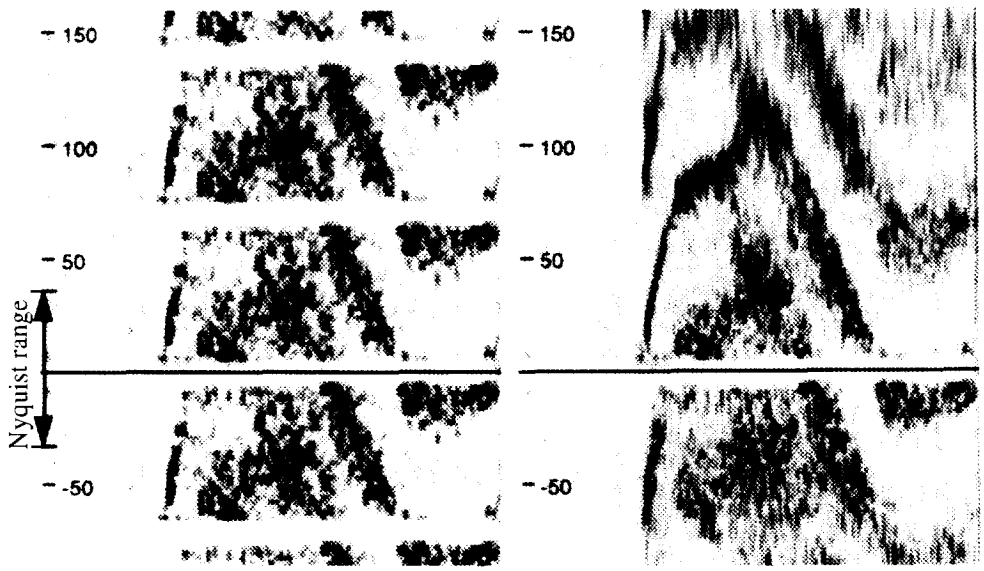

Fig. 6. VM spectrum analysis (right) compared to conventional spectrum analysis (left) applied to aortic artery flow with peak velocity at three times the Nyquist limit. Velocity labels are in centimeters per second.

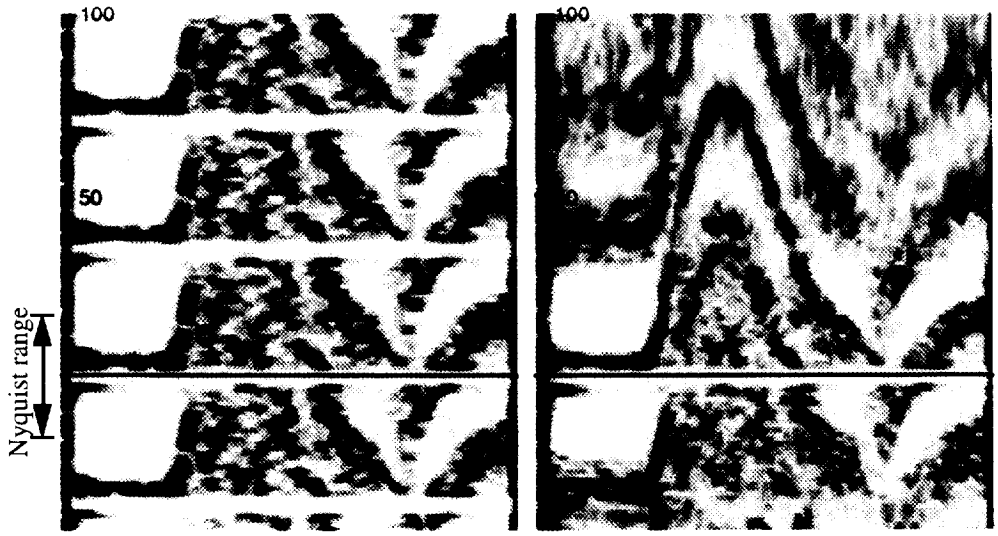

Fig. 7. VM spectrum analysis (right) compared to conventional spectrum analysis (left) applied to subclavian artery blood flow with peak velocity at 4.5 times the Nyquist limit. Velocity labels are in centimeters per second.

spectral energy in the signal, even when the center point is located inside the stop-band of the wall motion filter.

CONCLUSIONS

By applying a stochastic two-dimensional model for the received Doppler signal, the performance of the proposed algorithm "velocity matched spectrum" has been analyzed theoretically. The expressions for the expectation value of the spectrum estimators show that the VM-spectrum gives significant suppression of aliased grating lobes, and a narrower main lobe compared to the conventional spectrum algorithm. The VM spectrum has also been shown to give correct velocity calibration even in the case of frequency dependent attenuation. The experimental results show Doppler spectrum display with improved performance compared to the conventional method. Apart from suppression of aliased spectral components, the VM spectrum algorithm almost eliminates the wall motion filter dead zones, which helps the user in delineating the correct velocity waveform.

So far, the VM spectrum method has been analyzed and experimentally verified only for laminar flow with velocities up to 1.2 m/s. Velocity gradients inside the sample volume that occur in a typical high-velocity jet flow area, will limit the ability to resolve velocity ambiguity. However, when the core region of the high velocity jet is comparable with the sample volume size, the VM spectrum is expected to give significant improvements compared to conventional methods.

Acknowledgement—This work was supported by the Norwegian Research Council.

REFERENCES

Angelsen, B. A. J. A theoretical study of the scattering of ultrasound from blood. IEEE Trans. Biomed. Eng. BME-27:61–67; 1980.

Bonnefous, O.; Pesque, P. Time domain formulation of pulse-Doppler ultrasound and blood velocity estimation by cross-correlation. Ultrason. Imag. 8:73–85; 1986.

Ferrara, K.; Algazi, V. R. A new wideband spread target maximum likelihood estimator for blood velocity estimation. Part I: Theory. IEEE Trans. Ultrason. Ferroelec. Freq. Control UFFC-38:1–26; 1991.

Ferrara, K.; Algazi, V. R. The effect of frequency dependent scattering and attenuation on the estimation of blood velocity using ultrasound. IEEE Trans. Ultrason. Ferroelec. Freq. Control UFFC-39:754–767; 1992.

Iinuma, K. Doppler effect blood flow sensing device displaying signals lying within a band width related to sampling frequency. U.S. Patent No. 4,485,821; 1984.

Kristoffersen, K. Real time spectrum analysis in Doppler ultrasound blood velocity measurement. SINTEF report; 1984.

Mo, L. Y. L.; Cobbold, R. S. C. A unified approach to modeling the backscattered Doppler ultrasound from blood. IEEE Trans. Biomed. Eng. BME-39:450–461; 1992.

Oppenheim, A. V.; Schafer, R. W. Digital signal processing. New York: Prentice-Hall; 1975.

Torp, H.; Kristoffersen, K.; et al. Autocorrelation techniques in color flow imaging. Signal model and statistical properties of the autocorrelation estimates. IEEE Trans. Ultrasound Ferroelec. Freq. Control 41(5):604–612; 1994.

Wilson, L. S. Description of broadband pulsed Doppler ultrasonic processing using the two-dimensional Fourier transform. Ultrason. Imag. 13:301–315; 1991.